Shock-wave generation in transparent media from ultra-fast lasers

R. Bernath*[a], C. G. Brown[a], J. Aspiotis[a], M. Fisher[a], & M. Richardson[a]
[a]Laser Plasma Laboratory, College of Optics & Photonics: CREOL & FPCE,
University of Central Florida, 4000 Central Florida Blvd, Orlando, FL 32816-2700

ABSTRACT

Laser interactions with bulk transparent media have long been investigated for material processing applications involving ablation and shock wave generation in both the nanosecond and femtosecond pulse width regimes[1]. Shock waves have been studied in fused silica and other optical glasses but previously have been characterized by the morphology of the concurrent ablation. We perform ablation at distances of 30 meters using the non-linear self-channeling effect. Using silicon wafers as targets because of their clearly defined ablation zones, we examine the effect that the filament has on the thin SiO_2 layer coating the wafer's surface. It is observed that the surface layer experiences a shock wave resulting from the explosive forces produced by the plasma. The use of several laser pulses in burst mode operation leads to the observation of multiple shock fronts in the material, and the possibility of shock wave addition for higher damage. Optical interferometry will be used to characterize the shock wave dynamics, using both traditional means of focusing in the near field and at 30 meters using propagating self-channeled femtosecond pulses. The novelty of using self-channeling laser pulses for shock wave generation has many implications for military applications. These experiments are to be performed in our secure test range using intensities of 10^{14} W/cm^2 and higher incident on various transparent media. Interferometry is performed using a harmonic of the pump laser frequency. Experiments also include burst-mode operation, where a train of ultra-fast pulses, closely spaced in time, and novel new beam distributions, strike the sample.

Keywords: Femtosecond, ablation, shock waves, filamentation, laser plasma, interferometry

1. INTRODUCTION

Laser interactions with materials have been studied since the advent of the laser. Metals in the form of razor blades were used as a means of power measurement; then, as average laser powers increased, the ability to cut and weld metals for industrial purposes became apparent. As a result of the industrial applications much of the material interaction research has been performed on metals and focused on increasing cutting speeds and cut quality. The extensive knowledge base from this prior work is useful to our present study, since dielectrics behave similarly in terms of ablation.

Clean fabrication in metals has long been difficult with lasers due to the high thermal conductivity and low melting points typical of metals. With conventional lasers this has resulted in large heat-affected zones, non-uniform holes, and reformed molten surface debris. This is the result of working in the slow-pulse regime, with pulses greater in length than a nanosecond. Nolte *et al*[2] performed studies on the ablation of metals and dielectrics using femtosecond and picosecond pulses. A significant amount of the work was performed using 150–fs pulses from a Ti:sapphire laser at fluences of 0.1–10 J/cm^2. This resulted in the first characterization of separate ablation regimes as a function of laser pulse length. With this recognition came the ability to fabricate micro-structures on solid targets with better precision, decreased deposited energy, and less surface damage. Silicon (even though not a metal) and its compounds were studied due to the potential to laser-machine silicon wafers during semiconductor chip manufacturing. Using a Ti:sapphire laser at 790-nm wavelength with 130-fs pulses under vacuum, researchers have studied the ablation damage to the surface, including the structural details, in a fluence region above the damage threshold. From this it has been verified that at or just above the damage threshold, the silicon tends to melt, and at higher fluences it tends to follow into the ablation regime.[3]

*rbernat@creol.ucf.edu Phone: 407-823-6832 Fax: 407-823-6880

Enabling Technologies and Design of Nonlethal Weapons, edited by Glenn T. Shwaery, John G. Blitch, Carlton Land,
Proc. of SPIE Vol. 6219, 62190A, (2006) · 0277-786X/06/$15 · doi: 10.1117/12.663818

The two main regimes in laser ablation are the multi-photon (skin depth) and the electron diffusion (thermal) regimes. These come out of the Arrhenius-type evaporation equations,[4] and describe the ablation process by

$$L = \delta \ln\left(\frac{F_a}{F_{th}^{Skin}}\right) \text{ where } \delta \approx \alpha^{-1} \tag{1}$$

for irradiances below 10^{13} W/cm^2 and

$$L = l \ln\left(\frac{F_a}{F_{th}^{thermal}}\right) \text{ where } l \approx \sqrt{D\tau_a} \tag{2}$$

for irradiances above 10^{13} W/cm^2. These equations describe the effective ablation depth per shot in terms of the incident laser fluence. For low incident fluences, the skin depth (defined above as δ) defines the effective depth of absorption. For higher laser fluences, the electron thermal diffusion length (defined as *l*) dominates and increases the ablation rate over that of the skin depth regime. The advantage of the electron diffusion regime is that the laser energy goes directly into the generation of free electrons, thereby creating less heating of the surface and more ablation. This results from the laser pulse occurring for a time length shorter than the phonons can respond. For longer pulses, the phonons react and absorb the laser light directly as heat.

Femtosecond irradiation of solid material at 10^{14} W/cm^2 creates highly ionized plasma. This plasma has very high electron densities that can initially be higher than the solid's density. The high electron density and electron temperature result in a non-equilibrium state that begins to thermalize in times of ~1 ps after the laser pulse. About 100 ps later, the material expands and a small rarefaction wave propagates into the medium.[5] Sokolowski-Tinten et al. created a pressure versus density model derived from solid state models.[6] Their work was with aluminum irradiated at high intensities with electron temperatures approaching 30eV and pressures of tens of GPa. The pressure inside the plasma can increase to >100 GPa, with electron temperatures of tens of thousands of keV at irradiances greater than 10^{14} W/cm^2. However, this model does not take into account the hot electrons in the plasma, which also produce significant pressure and heating. MEDUSA[6], a hydrodynamic code, is used to model the electron temperature and density. Initial MEDUSA code calculations show that the laser pulse causes electron densities to increase by two orders of magnitude above the solid's density and produces temperatures of keV; this explains the generation of extremely high pressures. Using both the solid state and hydrodynamic models, it is possible to optimize the pressure and temperature to produce the largest possible shock waves.

2. ABLATION MODALITIES

Different irradiation modalities are considered for the generation of shock waves. We consider here two new modalities: the multiple pulse regime and the use of novel beam distributions. The multiple pulse regime derives from our extensive work on studying improved ablation rates and increasing laser absorption in various materials. For this work, we 'stack' between two and eight femtosecond pulses coaxially, with each pulse separated by ~ 4 ns. The result is a burst of laser pulses whose total energy can be higher than that of a single pulse. Figure 1 shows an illustration of the different shockwaves generated by single pulse, bursts of pulses, and beam distributions.

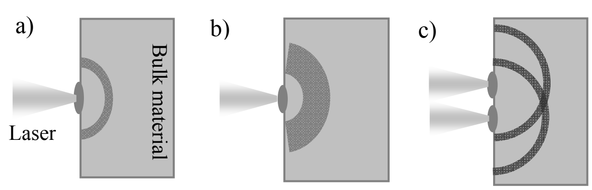

Fig 1. a) Single pulse shock front. b) Burst pulses and wider shock wave.
c) Two adjacent pulses and the intersection of their shock waves.

A single pulse generates a strong spherically expanding shock wave into the medium. Bursts of pulses with close temporal separation result in the plasma pressure remaining high, which is verified using MEDUSA code calculations, and generate a much wider shockwave. Shockwave addition is possible, since compression waves are additive, using multiple pulses separated spatially and allowing the expanding waves to overlap. The illustration is only two-dimensional but this can easily be performed in three dimensions using many parallel laser pulses. Novel spatial beam distributions are created using diffractive optical elements (DOE's). The DOE is inserted into the optical beam path prior to focusing onto the target and results in a designed beam spot distribution.

In addition, shockwaves have been generated at distances of 30 meters by the use of non-linear atmospheric propagation, commonly referred to as filamentation. Filamentation is the result of two competing processes occurring in the propagating medium, resulting in a stable channel of light that does not diverge. High-intensity laser pulses experience the standard index of refraction and the non-linear component dependant on the electric field amplitude. Laser beam self-focusing results from the electric field gradient across the beam and typically occurs for intensities greater than 10^{13} W/sr. At intensities of 10^{14} W/sr weak ionization of the air molecules generates free electrons that add a negative component to the refractive index. The two processes result in stable propagating filaments. However, there are limitations on how much energy per pulse can be transmitted in this fashion. Bursts of pulses and different beam distributions bypass some of these power limitations. DOE's can be used to generate multiple separate filaments in specific patterns. However, the number of filaments that can be created depends on the laser energy available, *i.e.*, each filament must contain at least the minimum intensity required for propagation.

3. EXPERIMENT

For these studies, we used the LPL Terawatt laser, a 10-TW-peak-power laser consisting of a Ti:sapphire oscillator followed by a multi-stage CPA Cr:LiSAF amplifier system. The oscillator is a 90-MHz Z-cavity design, tuned to 850-nm center wavelength, corresponding to the peak-gain wavelength of Cr:LiSAF. In the current configuration output pulses of ~110 femtoseconds in duration with energies up to 15 mJ/pulse were used. A portion of the beam prior to compression is used for second harmonic generation in a BBO crystal, which provides optical probing with pulses of 200 picosecond durations. The bursts of pulses are generated using a unique design of regenerative amplifier allowing the extraction of multiple pulses[8-9]. These are then spatially multiplexed in an interferometer, spacing them ~4 ns apart.

3.1. Lateral Shockwave Generation

The initial long-distance experiments were performed using silicon wafers as targets at the end of a 30-meter test range. These monocrystalline wafers are coated with a 200-nanometer protective layer of silicon dioxide. Single-pulse irradiance causes a delamination of the protective layer from the silicon substrate in the shape of the incident laser pulse, and a strong shockwave propagates out radially from the impact region. Due to the nature of the filamentation process, the beam distribution is always circular, which can be seen in figure 2a. The center gray area is only the substrate; the outer ring and surrounding area are silicon dioxide. The addition of subsequent pulses (burst pulses) creates individual delamination spots on the surface and separate shockwaves propagating within the coating layer. Non-circular regions are the result of multiple pulses overlapping on the surface. Figure 2b shows four pulses incident with two pulses overlapped in the left most region and two adjacent spots. The two small shapes between the first and second impacts are fractures in the silicon dioxide layer resulting from the intersection of the shockwaves from the first three pulses. The last pulse contained less energy than the previous three, which explains the absence of fractures between the middle and right spot.

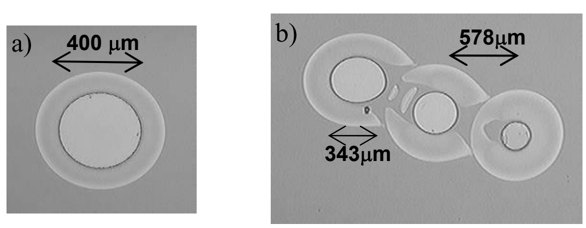

Fig 2. a) 12 mJ single pulse on silicon wafer.
b) Burst of pulses at 8 mJ each.

To investigate these fractures further, SEM images were taken of the samples along with TSL electron diffraction to determine the chemistry of the surface (specifically, the outer ring). On a different sample than shown above, the shockwave overlap caused stress buckling of the silicon dioxide layer as shown in figure 3.

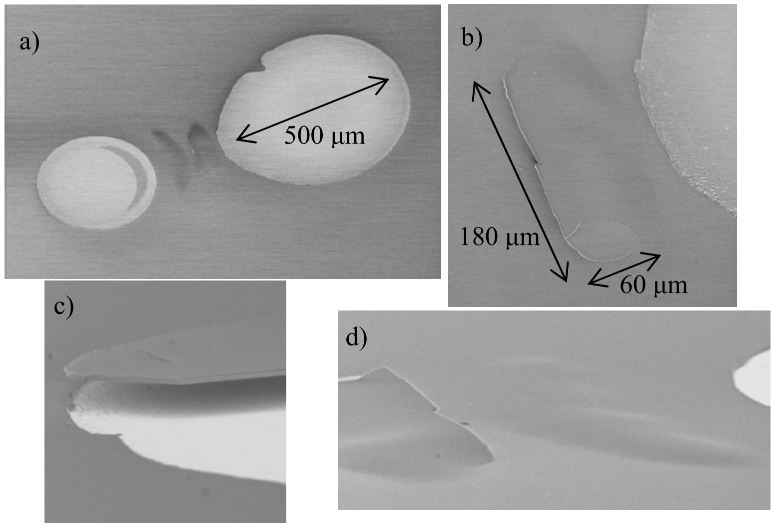

Fig 3. a) Multiple pulse shockwave. b) Close up of fracture from image c) Delamination of surface layer. d) Fractured region from figure 2b. Note the absence of the outer ring and any surface irregularities.

Under the highest magnification possible no physical signs were apparent of the outer ring. The electron diffraction suggested that there was not material difference between the unaffected areas and the darkened ring. Since the ring is only visible optically, this implies that the silicon dioxide layer underwent a material change. One possibility is an increase in the density caused by the shock wave. It has been observed in high-intensity nanosecond pulses incident on fused silica (i.e., fused silicon dioxide) that the density can increase up to 20% as a result of the shock[10]. Another possibility is a non-thermal melting of the surface, which has been observed in silicon and dielectrics. However, this requires further testing.

3.2. Optical Diagnosis of Longitudinal Shockwaves

Shock wave addition has been observed in surface waves; but, to observe this in longitudinal waves, a different geometry is required. This is to be accomplished by means of time-resolved optical interferometry utilizing the second harmonic beam from the laser system. A Wollaston prism is used to generate the interference pattern that will provide information regarding the plasma density and the shock wave intensity inside the material. An optical delay line provides time resolution at specific points in the shock wave's propagation.

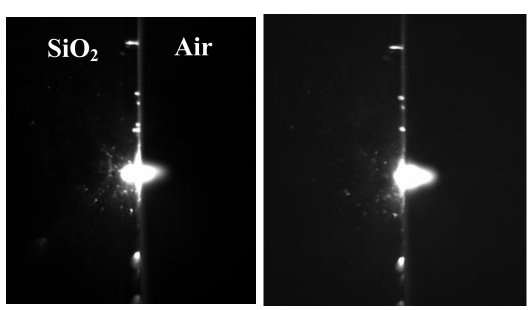

Fig 4. Images of the plasma formed on the fused silica. The laser is incident from the right and the boundary is the faint line in the middle.

The sample is a fused silica optical flat, about 1 mm thick, which is irradiated on edge. The probe beam will pass through the sample and record the density changes in the material and in the plasma. Initial experiments have been performed, recording the white light emission from the plasma with no probe beam. In figure 4, the faint line in the center of the images is the edge of the fused silica; the laser is incident from the right. The small lines seen above and below the plasma are reflections from the drilled holes in the silica caused by previous ablation. Using the modalities of shock wave generation described earlier, we hope to record the intensities of the shock fronts and additive regions inside the material.

4. CONCLUSIONS

Initial experiments using silicon wafers coated in SiO_2 showed signs of shock wave generation and additive shock waves in the surface material. This allows the possibility to custom-design shock waves using specific incident beam patterns such that the shock waves overlap at a specific point inside the material. In addition, bursts of pulses can cause much stronger damage on target by the subsequent shock waves generated. Future experiments will use optical interferometry to directly measure the intensity of the overlapped shock waves and will begin optimization of the interaction parameters.

ACKNOWLEDGEMENTS

We would like to thank Somsak (Tony) Teerawattanasook for his contributions and technical expertise. In addition, we would like to thank our colleagues for all their helpful advice during this project. This work is supported by the NTIC, the JNLWD (ORMC), ARO and the State of Florida.

REFERENCES

1. M. Kasaai, V. Kacham, F. Theberge, S. Chin, "The interaction of femtosecond and nanosecond laser pulses with the surface of glass," *J. Non-Crystalline Solids* **319** (2003) 129-135.
2. S. Nolte, B.N. Chichkov, H. Welling, Y Shani, K. Lieberman, H. Terkel, "Nanostructuring with spatially localized femtosecond laser pulses," *Opt. Lett*. 24, 914, 1999.
3. A. Borowiec, M. Mackenzie, G. C. Weatherly, H. K. Haugen, "Transmission and scanning electron microscopy studies of single femtosecond-laser-pulse ablation of silicon," *Applied Physics A*, **76**, 201-207, 2003.
4. S. Nolte, C. Momma, H. Jacobs, A. Tunnermann, B.N. Chichkov, B. Wellegehausen, H. Welling, "Ablation of metals by ultrafast laser pulses," *J. Opt. Soc. Am. B,* **14**, 2716, 1997.
5. B. Rethfeld, K. Sokolowski-Tinten, D. Von Der Linde, S. Anisimov, "Timescales in the response of materials to femtosecond laser excitation," *Applied Physics A*, 79, (2004) 767-769.
6. K. Sokolowski-Tinten, J. Bialkowski, A. Cavalleri, D. von der Linde, "Transient State of Matter during Short Pulse Laser Ablation," *Physical Review Letters*, Vol 81, No 1, (1998) 224-227.
7. J.P. Christiansen, D.E.T.F. Ashby, K.V. Roberts, "MEDUSA: A One- Dimensional Laser Fusion Code," *Comp. Phys. Comm*., 7, (1974), 271–287
8. M. Richardson, N. Vorobiev, A. Zoubir, N. Bernath, T. Olmstead, J. Duncan, "Burst Mode High Power Femtosecond Laser Propagation Through the Atmosphere," *Proceedings CLEO,* 2003**.**
9. P. Gonzales, R. Bernath, J. Duncan, T. Olmstead, M. Richardson, "Femtosecond ablation scaling for different materials," *Proceedings CLEO Europe*, Vol 5458, p 265-272, 2004.
10. A. Kubota, M. Caturla, J. Stolken, M. Feit, "Densification of fused silica due to shock waves and its implications for 351 nm laser induced damage," *Optics Express*, Vol 8 No 11, (2001) 611-616.